equations are not simultaneous. If the applied loads are constant in time, the equations have constant coefficients and the solutions can be put into exponential form. Otherwise a power series solution or a numerical procedure is necessary.

References

[1] Lin, T. H., "Creep Deflection of Viscoelastic Plate Under Uniform Edge Compression," *Journal of the Aeronautical Sciences*, Vol. 23, No. 9, Sept. 1956, pp. 883–887.

[2] DeLeeuw, S. L., and Mase, G. E., "Behavior of Viscoelastic Plates Under the Action of In-Plane Forces," *Proceedings of the Fourth U.S. National Congress of Applied Mechanics*, June, 1962, pp. 999–1005.

[3] Timoshenko, S., *Theory of Elastic Stability*, McGraw-Hill, New York, 1936.

[4] Biot, M. A., "Variational and Lagrangian Methods in Viscoelasticity," *International Union of Theoretical and Applied Mechanics Colloquium on Deformation and Flow of Solids*, Sept. 1955, pp. 251–263.

[5] Hildebrand, F. B., *Advanced Calculus for Engineers*, Prentice-Hall, New York, 1948.

[6] Mindlin, R. D., and Goodman, L. E., "Beam Vibrations with Time-Dependent Boundary Conditions," *Transactions of the American Society of Mechanical Engineers, Journal of Applied Mechanics*, Vol. 72, 1950, pp. 377–380.

[7] Galerkin, B., "Sur la Stabilité d'une Plaque Uniformément Comprimée Parallèlment a su Surface, Limitée par Deux Arcs de Cercles Concentriques et par Deux Rayons," *Comptes Rendus de L'Academie des Sciences*, Vol. 179, 1924, pp. 1392–1394.

[8] Meissner, E., "Ueber das Knicken Kreisringformiger Scheiben," *Schweizerische Bauzeitung*, Vol. 101, Feb. 1933, pp. 87–89.

[9] Timoshenko, S., *Strength of Materials*, Pt. II, Van Nostrand, New York, 1941.

[10] Galerkin, B., "Series Solutions of Some Problems of Elastic Equilibrium of Rods and Plates," *Vestnik Inzhenerov*, Vol. 1, 1915, pp. 879–908.

MAY 1971 AIAA JOURNAL VOL. 9, NO. 5

Stress Waves in Layered Thermoelastic Media Generated by Impulsive Energy Deposition

H. E. GASCOIGNE*
University of Utah, Salt Lake City, Utah

AND

I. K. McIVOR†
University of Michigan, Ann Arbor, Mich.

When high-intensity electromagnetic energy impinges on an elastic media, energy is deposited internally by photoelectric absorption and scattering. A spatially nonuniform heating is produced with deformation waves being generated in the media. The transient stresses resulting from such an energy deposition in an initially undisturbed layered media is investigated. The internal energy deposition is considered to be equivalent to an internal heat generation varying exponentially with the distance from the exposed surface. Energy is deposited internally according to a different law in each layer. The energy deposition is assumed to occur in a time negligible in comparison to a characteristic mechanical response time. Only spatial variations normal to the plane of the layers are considered. The equations of linear, uncoupled thermoelasticity, assuming constant material properties, are applied to a two-layer media. A boundary value problem is formulated and solved exactly neglecting heat conduction. Numerical examples are presented for several cases showing the effect of specific energy deposition functions, material thickness ratio, and material parameters. A complete description of interior stress reflection is presented. The influence of energy deposition and other material parameters on the interfacial bond stress is shown. Relatively small changes in layer parameters may have a marked effect on the maximum stress, depending on the manner in which the generated stress waves combine.

Introduction

MOST solids exhibit some opacity to electromagnetic radiation with energy being deposited in the media as a result of photoelectric absorption and scattering. Energy is propagated into the media at velocities comparable to the speed of light with, in some cases, a time pulse width such that deposition is complete in times on the order of 10^{-8} sec. This input time is substantially less than the time for an elastic dilatation wave to travel through the medium a characteristic distance. For metallic structures, using a characteristic length of 1 cm, this typical mechanical response time is on the order of 10^{-6} sec. The deposition of energy as a function of depth penetrated depends on the energy spectra of the radiation. The deposition (or absorption) law is an exponential decreasing function for monochromatic radiation.

Because of the extremely short-time duration of deposition, elastic deformation waves are generated. White[1] studied the effects of absorption of radiation created by high-power, pulsed light sources. Zaker[2] investigated elastic stress wave generation in an elastic half-space and in a homogeneous elastic slab caused by absorption of energy at microwave frequencies. Morland[3] studied the effect of electromagnetic absorption in an elastic half-space; Hegemier and Morland[4] investigated the effect in a viscoelastic half-space. No attempt has been made in these investigations to include the effect of nonhomogeneous media.

Many modern aerospace structures are composed of plate and shell-like sections formed as laminates with two or more layers of different materials. They are joined either by molecular bonding or by a bond with finite thickness and elasticity. Adhesion failure due to transient loading produc-

Received January 12, 1970; revision received July 6, 1970.

* Assistant Professor, Department of Mechanical Engineering.
† Professor, Department of Engineering Mechanics.

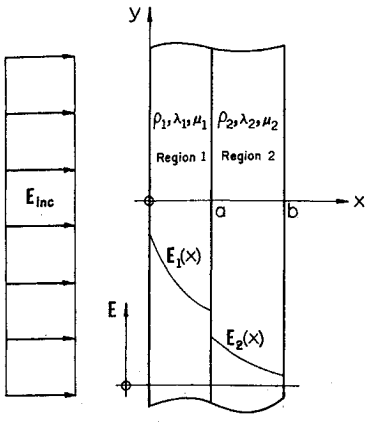

Fig. 1 Definition of coordinate system and energy deposition distribution.

ing large interface bond stresses may be extremely important in causing over-all structural failure. Goland and Reissner[5] were early investigators in bonded joints. Payton[6,7] investigated dynamic bond stresses in composite shells and rods subjected to sudden application of external loading.

The purpose of the present work is to determine the transient mechanical response of an initially undisturbed composite media formed by two-finite thickness plane layers with different material properties. These layers are joined by an interfacial molecular bond. The media is subjected to electromagnetic energy deposition uniformly over the lateral surface, with the deposition occurring in a time small compared with a defined mechanical response time. It is assumed that the lateral dimensions of the layered structure are large compared to its thickness. Edge effects are neglected. Hence, a one-dimensional representation is assumed accounting for variation through the thickness of the layered media. Considering the energy deposition as equivalent to a spatially varying internal heat source, the equations of linear thermoelasticity are applied to the layered media. A boundary value problem is formulated neglecting thermomechanical coupling and heat conduction. Thermomechanical coupling is neglected because of its generally small effect, and heat conduction is neglected based on the results obtained in Ref. 9.

A Laplace transform solution method is used because of the ease in which traveling discontinuities may be treated. The transform problem is solved for all values of time with the realization that only small time behavior will generally be valid because heat conduction is neglected. Numerical examples are presented for several cases showing the effect of specific energy deposition functions, material thickness ratio, and other material parameters. A complete description of interior stress reflection is presented. The interfacial bond stress is calculated because of its importance.

Governing Equations

The layered media, Fig. 1, is suddenly subjected to uniform normally incident electromagnetic energy flux E_{inc} per unit time impinging onto the surface at $x = 0$. In general, energy is deposited internally according to a different law in each layer resulting in a discontinuous deposition occurring at $x = a$, as shown in Fig. 1.

The governing equations follow from the well-known theory of linear thermoelasticity. Their derivation may be found in Ref. 8. Here we consider constrained uniaxial motion of the layered media. Thus the only nonzero displacement component is

$$u = u(x,t) \tag{1}$$

The only nonzero strain is

$$e_x(x,t) = [\partial u(x,t)]/\partial x \tag{2}$$

The corresponding nonzero stresses for a linearly elastic, isotropic material are

$$\sigma_x(x,t) = (\lambda + 2\mu)[\partial u(x,t)/\partial x] - (3\lambda + 2\mu)\alpha\theta(x,t) \tag{3}$$

$$\sigma_y(x,t) = \sigma_z(x,t) = \lambda[\partial u(x,t)/\partial x] - (3\lambda + 2\mu)\alpha\theta(x,t) \tag{4}$$

where λ and μ are the Lamé constants, α is the coefficient of thermal expansion, and θ is the temperature rise above the initial reference temperature. The appropriate values of the material constants are used for the two regions.

The equation of motion is

$$(\lambda + 2\mu)\frac{\partial^2 u(x,t)}{\partial x^2} - (3\lambda + 2\mu)\alpha\frac{\partial\theta(x,t)}{\partial x} = \rho\frac{\partial^2 u(x,t)}{\partial t^2} \tag{5}$$

where ρ is the mass density. Finally, neglecting heat conduction and thermomechanical coupling, the energy equation is

$$Q(x,t) = \rho S\partial\theta(x,t)/\partial t \tag{6}$$

where S is the specific heat at constant strain and Q is the internal heat generation. Equations (5) and (6) hold in each layer as shown in Fig. 1.

The deposition of energy is considered equivalent to internal heat generation:

$$Q_1(x,t) = E_1(x)g_1(t), \quad 0 \leq x < a, \; t > 0 \tag{7}$$

$$Q_2(x,t) = E_2(x)g_2(t), \quad a < x \leq b, \; t > 0 \tag{8}$$

As discussed, the time duration of deposition is small compared with a characteristic mechanical response time. Thus, it will be assumed that the time dependence can be adequately described by the delta function.

Since thermal conduction has been neglected, the determination of the temperature from Eq. (6) requires only the initial value of θ. Thus, the spatial distribution of temperature is specified completely by the heat generation. Here the initial temperature excess is taken as zero. Hence,

$$\theta_1(x,0) = 0, \quad 0 \leq x < a \tag{9}$$

$$\theta_2(x,0) = 0, \quad a < x \leq b \tag{10}$$

The mechanical boundary conditions are those of traction-free surfaces at $x = 0,b$. They are

$$\sigma_{x1}(0,t) = 0, \quad t \geq 0 \tag{11}$$

and

$$\sigma_{x2}(b,t) = 0, \quad t \geq 0 \tag{12}$$

where the subscripts 1 and 2 refer to the appropriate region. Using Eq. (3), Eqs. (11) and (12) become, respectively,

$$(\lambda + 2\mu)_1[\partial u_1(0,t)/\partial x] - (3\lambda + 2\mu)_1\alpha_1\theta_1(0,t) = 0, \quad t \geq 0 \tag{13}$$

and

$$(\lambda + 2\mu)_2[\partial u_2(b,t)/\partial x] - (3\lambda + 2\mu)_2\alpha_2\theta_2(b,t) = 0, \quad t \geq 0 \tag{14}$$

Continuity of normal stress and displacement must hold at the interface. Thus,

$$(\lambda + 2\mu)_1\frac{\partial u_1(a,t)}{\partial x} - (3\lambda + 2\mu)_1\alpha_1\theta_1(a,t) = (\lambda + 2\mu)_2\frac{\partial u_2(a,t)}{\partial x} - (3\lambda + 2\mu)_2\alpha_2\theta_2(a,t), \quad t \geq 0 \tag{15}$$

$$u_1(a,t) = u_2(a,t), \quad t \geq 0 \tag{16}$$

The mechanical initial conditions are those for a quiescent media, namely

$$u_1(x,0) = 0, \quad 0 \leq x \leq a \tag{17}$$

$$u_2(x,0) = 0, \quad a \leq x \leq b \tag{18}$$

$$\partial u_1(x,0)/\partial t = 0, \quad 0 \leq x \leq a \tag{19}$$

$$\partial u_2(x,0)/\partial t = 0, \quad a \leq x \leq b \tag{20}$$

Eqs. (5), (6), and (11–20) completely specify the problem.

Solution

Transform Problem

The Laplace transform is used to suppress time in the aforementioned equations. The Laplace transform of a quantity will be denoted by an asterisk, for example,

$$f^*(x,s) = L[f(x,t)] = \int_0^\infty f(x,t)e^{-st}dt \tag{21}$$

The corresponding inverse transform is

$$f(x,t) = \frac{1}{2\pi i}\int_{Br} f^*(x,s)e^{st}ds \tag{22}$$

where s is the transform parameter and Br is the Bromwich contour in the right half of the s-plane. The transforms of Eqs. (5) and (6), after applying the initial conditions, are

$$\theta_1^*(x,s) = [Q_1^*(x,s)/(\rho S)_1]1/s, \quad 0 \le x < a \tag{23}$$

$$\theta_2^*(x,s) = [Q_2^*(x,s)/(\rho S)_2]1/s, \quad a < x \le b \tag{24}$$

$$\frac{d^2u_1^*(x,s)}{dx^2} - \frac{s^2}{c_1^2}u_1^*(x,s) = \Lambda_1\frac{d\theta_1^*(x,s)}{dx}, \quad 0 \le x < a \tag{25}$$

$$\frac{d^2u_2^*(x,s)}{dx^2} - \frac{s^2}{c_2^2}u_2^*(x,s) = \Lambda_2\frac{d\theta_2^*(x,s)}{dx}, \quad a < x \le b \tag{26}$$

where

$$c_i^2 = (\lambda + 2\mu)_i/\rho_i, \quad (i = 1,2)$$
$$\Lambda_i = [(3\lambda + 2\mu)_i\alpha_i]/(\lambda + 2\mu)_i, \quad (i = 1,2) \tag{27}$$

Transforming the boundary and continuity conditions, Eqs. (13–16) yield

$$[du_1^*(0,s)/dx] - \Lambda_1\theta_1^*(0,s) = 0 \tag{28}$$

$$[du_2^*(b,s)/dx] - \Lambda_2\theta_2^*(b,x) = 0 \tag{29}$$

$$[du_1^*(a,s)/dx] - \Lambda_1\theta_1^*(a,s) = \Lambda_3[du_2^*(a,s)/dx] - \Lambda_4\theta_2^*(a,s) \tag{30}$$

$$u_1^*(a,s) = u_2^*(a,s) \tag{31}$$

where

$$\Lambda_3 = (\lambda + 2\mu)_2/(\lambda + 2\mu)_1, \quad \Lambda_4 = (3\lambda + 2\mu)_2\alpha_2/(\lambda + 2\mu)_1 \tag{32}$$

Delta function time dependence is taken in Eqs. (7) and (8). With this, Eqs. (23) and (24) become

$$\theta_1^*(x,s) = [E_1(x)/(\rho S)_1]1/s, \quad 0 \le x < a \tag{33}$$

$$\theta_2^*(x,s) = [E_2(x)/(\rho S)_2]1/s, \quad a < x \le b \tag{34}$$

where $E_1(x)$ and $E_2(x)$ are the total energy distributions per unit volume deposited in layers 1 and 2, respectively. In general, for electromagnetic energy with a wavelength spectrum, the depth of penetration increases with decreasing wavelength. This effect can be approximated by taking the energy distribution functions as a sum of exponential functions, i.e.,

$$E_1(x) = E_{10}e^{-\gamma_{10}x} + E_{11}e^{-\gamma_{11}x} + \ldots = \sum_{m=0}^{M} E_{1m}e^{-\gamma_{1m}x}, \quad 0 \le x < a \tag{35}$$

$$E_2(x) = E_{20}e^{-\gamma_{20}(x-a)} + E_{21}e^{-\gamma_{21}(x-a)} + \ldots = \sum_{n=0}^{N} E_{2n}e^{-\gamma_{2n}(x-a))}, \quad a < x \le b \tag{36}$$

For convenience, a solution will be obtained for a one-term representation of Eqs. (35) and (36). More general solutions are obtained by superposition. The total energy distributions are

$$E_1(x) = E_1e^{-\gamma_1x}, \quad 0 \le x < a \tag{37}$$

$$E_2(x) = E_2e^{-\gamma_2(x-a)}, \quad a < x \le b \tag{38}$$

With this Eqs. (33) and (34) are

$$\theta_1^*(x,s) = [E_1e^{-\gamma_1x}/(\rho S)_1]1/s, \quad 0 \le x < a \tag{39}$$

$$\theta_2^*(x,s) = [E_2e^{-\gamma_2(x-a)}/(\rho S)_2]1/s, \quad a < x \le b \tag{40}$$

With the transformed temperatures known, the problem is reduced to solving Eqs. (25) and (26), subject to the boundary and continuity conditions (28–31).

Solution of the Transform Problem

The solutions of Eqs. (25) and (26) are

$$u_1^*(x,s) = E(s)e^{(s/c_1)x} + F(s)e^{-(s/c_1)x} + \frac{\Lambda_1E_1\gamma_1c_1^2e^{-\gamma_1x}}{(\rho S)_1}\frac{1}{s(s^2 - c_1^2\gamma_1^2)} \tag{41}$$

$$u_2^*(x,s) = G(s)e^{(s/c_2)x} + H(s)e^{-(s/c_2)x} + \frac{\Lambda_2E_2\gamma_2c_2^2e^{-\gamma_2(x-a)}}{(\rho S)_2}\frac{1}{s(s^2 - c_2^2\gamma_2^2)} \tag{42}$$

where $E(s)$, $F(s)$, $G(s)$, and $H(s)$ are determined from the boundary and continuity conditions.

The transformed stresses may be expressed in terms of these coefficients. Transforming Eq. (3) gives

$$\sigma_{x1}^*(x,s) = (\lambda + 2\mu)_1[du_1^*(x,s)/dx] - (3\lambda + 2\mu)_1\alpha_1\theta_1^*(x,s) \tag{43}$$

Using Eq. (39) and Eq. (41) gives the transformed stress as

$$\sigma_{x1}^*(x,s) = (\lambda + 2\mu)_1\left[\frac{s}{c_1}Ee^{(s/c_1)x} - \frac{s}{c_1}Fe^{-(s/c_1)x} - \frac{\Lambda_1c_1^2E_1\gamma_1^2e^{-\gamma_1x}}{(\rho S)_1}\frac{1}{s(s^2 - c_1^2\gamma_1^2)}\right] - (3\lambda + 2\mu)_1\alpha_1\left[\frac{E_1e^{-\gamma_1x}}{(\rho S)_1}\frac{1}{s}\right] \tag{44}$$

Similarly

$$\sigma_{x2}^*(x,s) = (\lambda + 2\mu)_2\left[\frac{s}{c_2}Ge^{(s/c_2)x} - \frac{s}{c_2}He^{-(s/c_2)x} - \frac{\Lambda_2c_2^2E_2\gamma_2^2e^{-\gamma_2(x-a)}}{(\rho S)_2}\frac{1}{s(s^2 - c_2^2\gamma_2^2)}\right] - (3\lambda + 2\mu)_2\alpha_2\left[\frac{E_2e^{-\gamma_2(x-a)}}{(\rho S)_2}\frac{1}{s}\right] \tag{45}$$

Once the coefficients E, F, G, and H have been determined, the stresses are obtained from the inversion of Eqs. (44) and (45).

The calculation of these coefficients is algebraically lengthy. Although for brevity the details, which may be found in Ref. 9, are omitted here, the success of the present method depends upon the form in which these coefficients are expressed. When the system of equations obtained from the boundary and continuity conditions is solved, the coefficients appear in fractional form. The denominator is simply the determinant of the coefficients of the system of equations. After some manipulation this denominator can be expanded in an exponential series. When the coefficients are introduced into Eqs. (44) and (45) in this expanded form, the transformed stresses can be expressed as a sum of a number of terms, each term in the form of an exponential series.

The complete expressions for the transformed stresses are given in Ref. 9. A typical term in these expressions is

$$\sigma_{x1}^*(x,s) = -(\lambda + 2\mu)_1\left[\frac{\Lambda_1E_1}{(\rho S)_1}\frac{1}{s} + \frac{\Lambda_1c_1^2E_1\gamma_1^2}{(\rho S)_1}\frac{1}{s(s^2 - c_1^2\gamma_1^2)}\right]\Sigma e^{-(2\beta_0 + j\beta_1 + k\beta_2 + l\beta_3 - (x/c_1))s} + \ldots \tag{46}$$

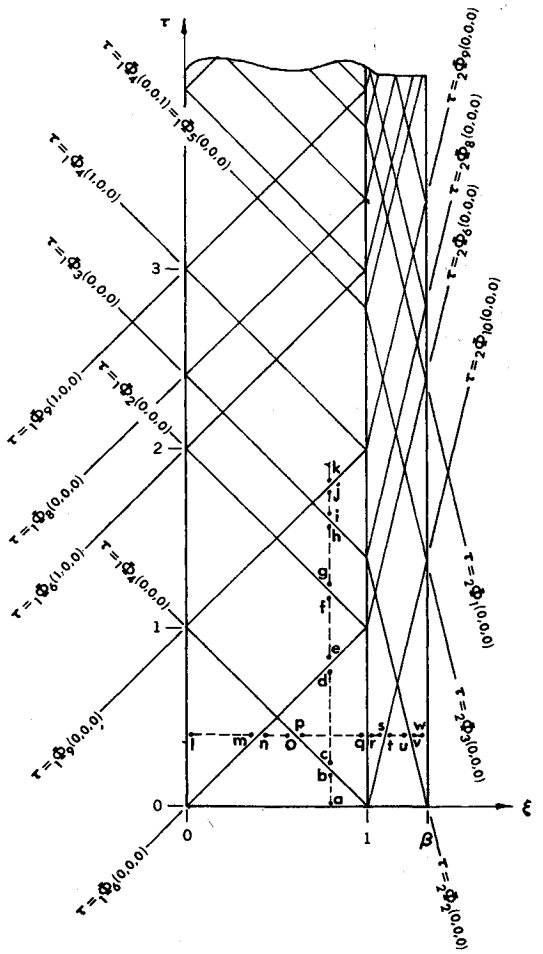

Fig. 2 ξ-τ solution space.

where

$$\beta_0 = (a/c_1) + [(b-a)/c_2], \quad \beta_1 = 2a/c_1$$
$$\beta_2 = (2a/c_1) + [2(b-a)/c_2], \quad \beta_3 = 2(b-a)/c_2 \tag{47}$$

The symbol Σ represents a summation operator defined as

$$\Sigma = \sum_{i=0}^{\infty} \sum_{\substack{j,k,l=0 \\ (j+k+l=i)}}^{i} \frac{i!}{j!\,k!\,l!} \left(\frac{1-z_{21}}{1+z_{21}}\right)\left(\frac{z_{21}-1}{z_{21}+1}\right)^{l} \tag{48}$$

where z_{21} is the ratio of the acoustic impedance of media two to media one, i.e.,

$$z_{21} = \rho_2 c_2/\rho_1 c_1 \tag{49}$$

The essential feature of Eq. (46) is that each term is a simple algebraic function of s times a series of exponentials.

Inverse Transform

The inverse transforms of Eqs. (44) and (45) are obtained by using the shift property of the Laplace transform, i.e. $L^{-1}[f(s)e^{-\phi s}] = F(t-\phi)H(t-\phi)$, where ϕ is a positive constant, $H(t-\phi)$ is the shifted step function defined by

$$H(t-\phi) = \begin{pmatrix} 0, & t < \phi \\ 1, & t > \phi \end{pmatrix}$$

and $F(t)$ is the inverse transform of $f(s)$. The functions for which inverse transforms are needed in evaluating Eqs. (44) and (45) are of the form $1/s$, $1/(s^2-a^2)$, and $1/s(s^2-b^2)$. They are listed in any standard book on operational calculus, for example, Ref. 10.

It is convenient to introduce the nondimensional quantities:

$$\xi = x/a, \quad \tau = (c_1/a)t, \quad \Gamma_1 = \gamma_1 a, \quad \Gamma_2 = \gamma_2 a$$
$$\sigma_{\xi 1}(\xi,\tau) = \sigma_{x1}(x,t)/[(3\lambda+2\mu)_1\alpha_1 E_1/(\rho S)_1]$$
$$\sigma_{\xi 2}(\xi,\tau) = \sigma_{x2}(x,t)/[(3\lambda+2\mu)_2\alpha_2 E_2/(\rho S)_2]$$
$$r = c_1/c_2, \quad \beta = b/a \tag{50}$$
$$K = [(3\lambda+2\mu)_2\alpha_2/(3\lambda+2\mu)_1\alpha_1]\{[E_2/(\rho S)_2]/[E_1(\rho S)_1]\}$$
$${}_p\Phi_q = {}_p\Phi_q(j,k,l,r,\beta,\xi), \quad (p = 1,2;\ q = 1,\ldots 10)$$

where ${}_p\Phi_q$ is listed in the Appendix. With the abbreviations ch and sh denoting, respectively, the hyperbolic cosine and sine, the inverse transform of Eqs. (44) and (45) are

$$\sigma_{\xi 1}(\xi,\tau) = -\Sigma\ \mathrm{ch}\Gamma_1(\tau - {}_1\Phi_1)H(\tau - {}_1\Phi_1) -$$
$$\frac{(1-z_{21})}{(1+z_{21})}\Sigma\ \mathrm{ch}\Gamma_1(\tau - {}_1\Phi_2)H(\tau - {}_1\Phi_2) +$$
$$\frac{2}{(1+z_{21})} K\Sigma e^{-\Gamma_2(\beta-1)}\left[1 + \mathrm{sh}\frac{\Gamma_2}{r}(\tau - {}_1\Phi_3)\right]H(\tau - {}_1\Phi_3) +$$
$$\frac{1}{(1+z_{21})}\Sigma\left\{e^{-\Gamma_1}[\mathrm{ch}\Gamma_1(\tau - {}_1\Phi_4) - z_{21}\,\mathrm{sh}\Gamma_1(\tau - {}_1\Phi_4)] + K\left[\mathrm{sh}\frac{\Gamma_2}{r}(\tau - {}_1\Phi_4) - \mathrm{ch}\frac{\Gamma_2}{r}(\tau - {}_1\Phi_4)\right]\right\}H(\tau - {}_1\Phi_4) +$$
$$\frac{1}{(1+z_{21})}\Sigma\left\{e^{-\Gamma_1}[\mathrm{ch}\Gamma_1(\tau - {}_1\Phi_5) + z_{21}\,\mathrm{sh}\Gamma_1(\tau - {}_1\Phi_5)] - K\left[\mathrm{sh}\frac{\Gamma_2}{r}(\tau - {}_1\Phi_5) + \mathrm{ch}\frac{\Gamma_2}{r}(\tau - {}_1\Phi_5)\right]\right\}H(\tau - {}_1\Phi_5) +$$
$$\Sigma\ \mathrm{ch}\Gamma_1(\tau - {}_1\Phi_6)H(\tau - {}_1\Phi_6) +$$
$$\frac{(1-z_{21})}{(1+z_{21})}\Sigma\mathrm{ch}\Gamma_1(\tau - {}_1\Phi_7)H(\tau - {}_1\Phi_7) -$$
$$\frac{2}{(1+z_{21})} K\Sigma e^{-\Gamma_2(\beta-1)}\left[1 + \mathrm{sh}\frac{\Gamma_2}{r}(\tau - {}_1\Phi_8)\right]H(\tau - {}_1\Phi_8) -$$
$$\frac{1}{(1+z_{21})}\Sigma\left\{e^{-\Gamma_1}[\mathrm{ch}\Gamma_1(\tau - {}_1\Phi_9) - z_{21}\mathrm{sh}\Gamma_1(\tau - {}_1\Phi_9)] + K\left[\mathrm{sh}\frac{\Gamma_2}{r}(\tau - {}_1\Phi_9) - \mathrm{ch}\frac{\Gamma_2}{r}(\tau - {}_1\Phi_9)\right]\right\}H(\tau - {}_1\Phi_9) -$$
$$\frac{1}{(1+z_{21})}\Sigma\left\{e^{-\Gamma_1}[\mathrm{ch}\Gamma_1(\tau - {}_1\Phi_{10}) + z_{21}\,\mathrm{sh}\Gamma_1(\tau - {}_1\Phi_{10})] - K\left[\mathrm{sh}\frac{\Gamma_2}{r}(\tau - {}_1\Phi_{10}) + \mathrm{ch}\frac{\Gamma_2}{r}(\tau - {}_1\Phi_{10})\right]\right\}H(\tau - {}_1\Phi_{10}) -$$
$$e^{-\Gamma_1\xi}\,\mathrm{ch}\Gamma_1\tau \tag{51}$$

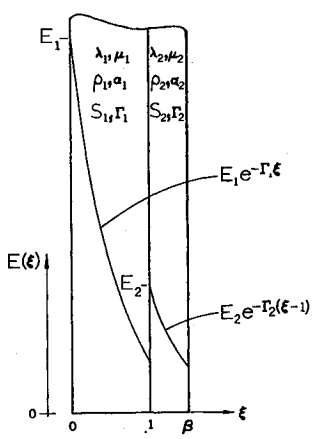

$$K = \frac{(3\lambda+2\mu)_2\alpha_2}{(3\lambda+2\mu)_1\alpha_1}\frac{E_2/(\rho S)_2}{E_1/(\rho S)_1} = 0.57$$

$\beta = 1.5, 1.25;\ \Gamma_1 = \Gamma_2 = 2;\ \Gamma = 7.35;\ z_{21} = 0.2$

Fig. 3 Energy deposition distribution for example problem.

$$\sigma_{\xi 2}(\xi,\tau) = -\frac{2z_{21}}{(1+z_{21})}\Sigma\,\mathrm{ch}\Gamma_1(\tau - {}_2\Phi_1)H(\tau - {}_2\Phi_1) +$$
$$K\Sigma e^{-\Gamma_2(\beta-1)}\,\mathrm{ch}\frac{\Gamma_2}{r}(\tau - {}_2\Phi_2)H(\tau - {}_2\Phi_2) -$$
$$\frac{(1-z_{21})}{(1+z_{21})}K\Sigma e^{-\Gamma_2(\beta-1)}\,\mathrm{ch}\frac{\Gamma_2}{r}(\tau - {}_2\Phi_3)H(\tau - {}_2\Phi_3) +$$
$$\frac{z_{21}}{(1+z_{21})}\Sigma\left\{e^{-\Gamma_1}[\mathrm{ch}\Gamma_1(\tau - {}_2\Phi_4) - \mathrm{sh}\Gamma_1(\tau - {}_2\Phi_4)] + K\left[z_{21}^{-1}\,\mathrm{sh}\frac{\Gamma_2}{r}(\tau - {}_2\Phi_4) - \mathrm{ch}\frac{\Gamma_2}{r}(\tau - {}_2\Phi_4)\right]\right\}H(\tau - {}_2\Phi_4) +$$
$$\frac{z_{21}}{(1+z_{21})}\Sigma\left\{e^{-\Gamma_1}[\mathrm{ch}\Gamma_1(\tau - {}_2\Phi_5) + \mathrm{sh}\Gamma_1(\tau - {}_2\Phi_5)] - K\left[z_{21}^{-1}\,\mathrm{sh}\frac{\Gamma_2}{r}(\tau - {}_2\Phi_5) + \mathrm{ch}\frac{\Gamma_2}{r}(\tau - {}_2\Phi_5)\right]\right\}H(\tau - {}_2\Phi_5) +$$
$$\frac{2z_{21}}{(1+z_{21})}\Sigma\,\mathrm{ch}\Gamma_1(\tau - {}_2\Phi_6)H(\tau - {}_2\Phi_6) -$$
$$K\Sigma e^{-\Gamma_2(\beta-1)}\,\mathrm{ch}\frac{\Gamma_2}{r}(\tau - {}_2\Phi_7)H(\tau - {}_2\Phi_7) +$$
$$\frac{(1-z_{21})}{(1+z_{21})}K\Sigma e^{-\Gamma_2(\beta-1)}\,\mathrm{ch}\frac{\Gamma_2}{r}(\tau - {}_2\Phi_8)H(\tau - {}_2\Phi_8) -$$
$$\frac{z_{21}}{(1+z_{21})}\Sigma\left\{e^{-\Gamma_1}[\mathrm{ch}\Gamma_1(\tau - {}_2\Phi_9) - \mathrm{sh}\Gamma_1(\tau - {}_2\Phi_9)] + K\left[z_{21}^{-1}\,\mathrm{sh}\frac{\Gamma_2}{r}(\tau - {}_2\Phi_9) - \mathrm{ch}\frac{\Gamma_2}{r}(\tau - {}_2\Phi_9)\right]\right\}H(\tau - {}_2\Phi_9) -$$
$$\frac{z_{21}}{(1+z_{21})}\Sigma\left\{e^{-\Gamma_1}[\mathrm{ch}\Gamma_1(\tau - {}_2\Phi_{10}) + \mathrm{sh}\Gamma_1(\tau - {}_2\Phi_{10})] - K\left[z_{21}^{-1}\,\mathrm{sh}\frac{\Gamma_2}{r}(\tau - {}_2\Phi_{10}) + \mathrm{ch}\frac{\Gamma_2}{r}(\tau - {}_2\Phi_{10})\right]\right\}\times$$
$$H(\tau - {}_2\Phi_{10}) - Ke^{-\Gamma_2(\xi-1)}\,\mathrm{ch}\frac{\Gamma_2}{r}\tau \quad (52)$$

Discussion of Solution

The solution for the stress as given by Eqs. (51) and (52) has a simple and convenient interpretation. There are in each of these equations eleven terms. Ten of these contain the unit step function and consequently make no contribution unless their argument is positive. The argument of these step functions differ by integral multiples of the time required for a dilation wave to traverse a given layer. Thus, as time proceeds, the various terms can be identified in a systematic manner as reflected waves. If the values of ${}_p\Phi_q$ in Eqs. (51) and (52) are displayed in a ξ-τ solution space, a typical result is shown in Fig. 2. In this diagram, particular values of $b/a = 1.33$ and $c_1/c_2 = 4$ have been used.

The method of determining the stresses $\sigma_{\xi 1}$ and $\sigma_{\xi 2}$ as a function of τ for a particular value of ξ is shown best by an example. A typical value ξ is indicated by the dashed line $a, b, c, \ldots$ in Fig. 2. At point a the only nonzero term of Eq. (51) is the last one when $\tau = 0^+$. Because of the delta function time dependence for the heat generation rate, the stress jumps to a finite value at $\tau = 0^+$. At point b, a value of τ slightly smaller than ${}_1\Phi_4$ (0,0,0), $\sigma_{\xi 1}$ is still given by the last term of Eq. (51). At $\tau = c$, a jump in stress is given by the fourth term of Eq. (51) by virtue of the positive argument of the step function $H(\tau - {}_1\Phi_4)$. From points c to d there are two nonzero terms, the tenth and the fourth. At point e, the sixth term creates a second jump because of the positive argument of the step function $H(\tau - {}_1\Phi_6)$. Between points e and f there are three nonzero terms, the tenth, the fourth, and the sixth. As the time τ increases, successive step functions become nonzero and the corresponding terms multiplied by them make a contribution. In each term, the series is evaluated for the values of j, k, and l associated with the particular ${}_p\Phi_q$ in question. For example, the value of the series Σ for the term corresponding to ${}_1\Phi_4$ (0,0,0) is 1; for the term corresponding ${}_1\Phi_4(1,0,0)$ it is $(1 - z_{21})/(1 + z_{21})$, and for the term corresponding to ${}_1\Phi_4(0,0,1)$ it is $-(1 - z_{21})/(1 + z_{21})$.

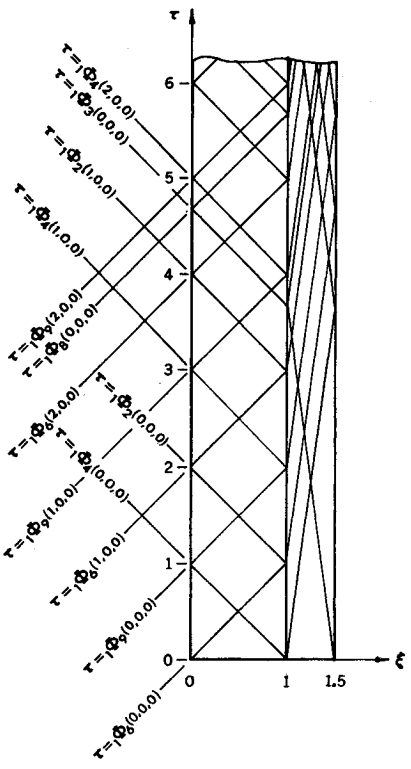

Fig. 4 ξ-τ solution space for example with $\beta = 1.5$; parameters are given in Fig. 3.

Calculating the stress as a function of the spatial coordinate ξ for a fixed value of τ is accomplished in a similar way. The σ_ξ stress at $\xi = 1$ (bond stress) may be calculated from either Eq. (51) or Eq. (52) by virtue of the continuity of σ_ξ at $\xi = 1$.

Numerical Examples

The case of the homogeneous slab of finite thickness was discussed in Ref. 2 and that of the homogeneous half-space was presented in Ref. 3. These cases may be obtained from the previous analysis as limiting cases. The examples considered here will be for the two-layer media.

The parameters used for the numerical example are shown in Fig. 3. The wave-speed ratio and the specific acoustic impedance ratio are sufficiently different to show a wide range of effects. The ratio of energy absorption at $\xi = 1$ expressed by $(E_1/E_2)_{\xi=1}$ is taken to be 0.4, with the other parameters chosen to give the value of $K = 0.57$. The ξ-τ solution space for a value of $\beta = 1.5$ is shown in Fig. 4. The maximum nondimensional tensile stress in the front layer is 0.43 and occurs at $\xi = 0.5^-$, due to the tensile jump of unit magnitude across $\tau = {}_1\Phi_6$ (0,0,0). In this case, the stress jump across $\tau = {}_1\Phi_4$ (0,0,0) is compressive and hence, combines to give a substantially reduced tensile stress at $\xi = 0.5$. Figure 5 shows the stress at $\xi = 0.1$–0.4, $\xi = 0.5^-$ and at $\xi = 0.5^+$. Figure 6 shows the stress at $\xi = 0.5$ (which is not the location of maximum tensile stress) as well as the bond stress at $\xi = 1$.

Changing the thickness ratio β may have a significant effect. Decreasing β will create the possibility of a higher peak tensile stress in the front layer. The magnitude of the increase depends upon the value of β. Fig. 7 shows the ξ-τ solution space for $\beta = 1.25$. In the front layer the jump across $\tau = {}_1\Phi_3$ (0,0,0) at $\xi = 0.5$ now occurs at $\tau = 2.33$.

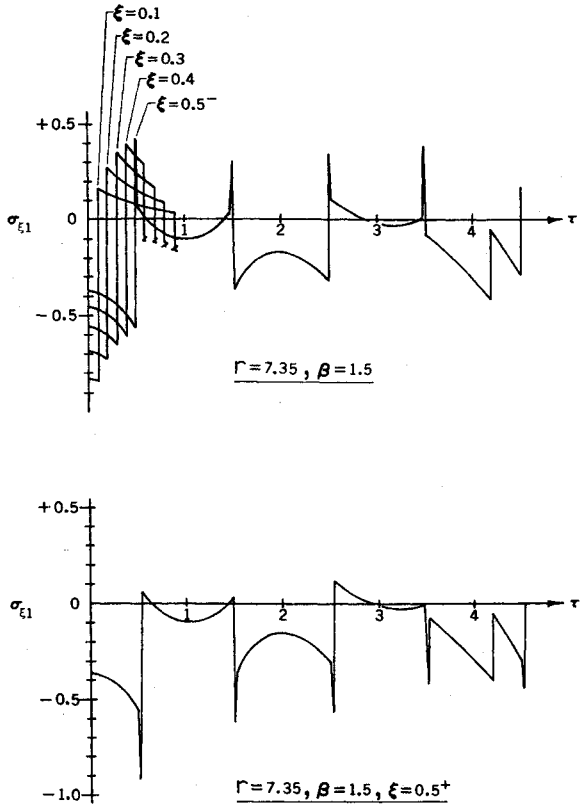

Fig. 5 Nondimensional stress vs nondimensional time for example. $\xi = 0.5$ is the middle plane of front layer.

This creates a substantial difference in the maximum tensile stress there. Figure 8 shows the stress at $\xi = 0.5$ and the bond stress at $\xi = 1$ for this case. The peak tensile bond stress has been sngificantly increased in the time interval $\tau < 4$.

Summary and Conclusions

The transient mechanical response of a layered media due to impulsive energy deposition has been analyzed. The media is formed by two elastic, homogeneous and isotropic plane layers joined by an interface molecular bond. A one-dimensional formulation has resulted from nelgecting in-plane strain components. The equations of linear thermoelasticity, assuming temperature independent properties, have been solved retaining inertia and neglecting thermomechanical coupling and heat conduction.

A solution for the stresses has been developed which is valid for all values of time. The present investigation provides a

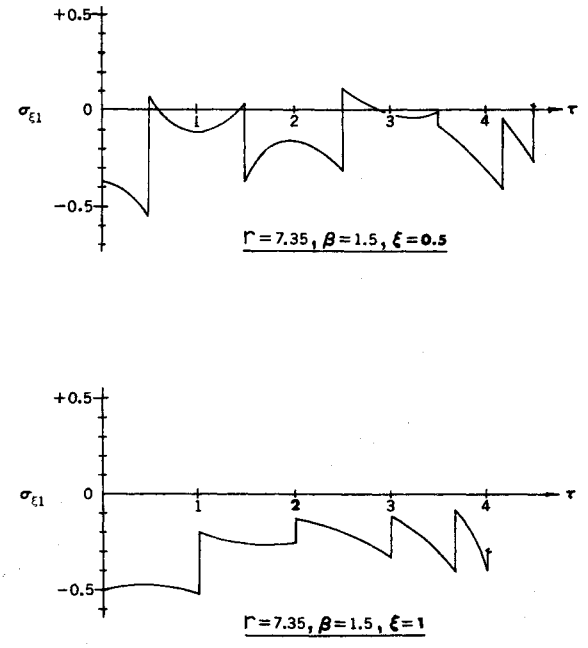

Fig. 6 Nondimensional stress vs nondimensional time for example. $\xi = 0.5$ is midplane of front layer (top); $\xi = 1$ is bond plane (bottom).

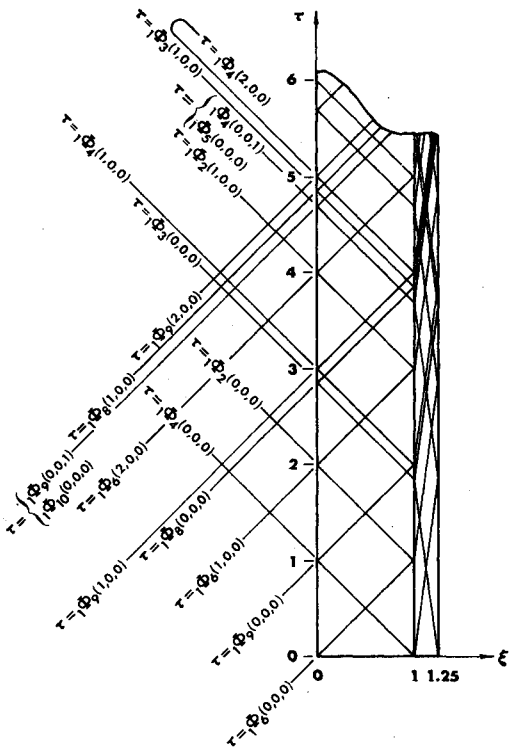

Fig. 7 ξ-τ solution space for example with $\beta = 1.25$; parameters are given in Fig. 3.

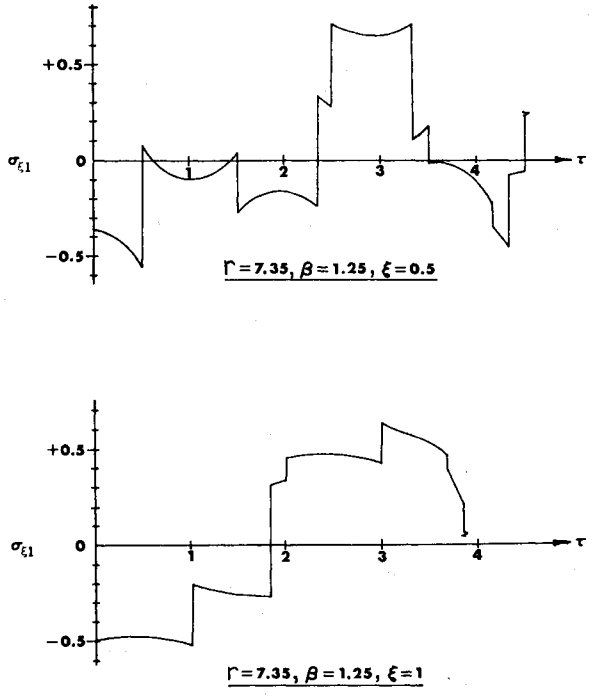

Fig. 8 Nondimensional stress vs nondimensional time for example. $\xi = 0.5$ is midplane of front layer (top); $\xi = 1$ is bond plane (bottom).

systematic method of accounting for multiple reflections in the media.

The magnitude of the maximum stress in the layer material and at the bond line depends on the thickness and wave-speed ratios of the layered media for given energy deposition functions. The maximum layer stress (or bond stress) depends markedly upon the manner in which the generated stress waves combine to either reinforce or cancel. This suggests that a stress optimization procedure may be developed in a specific application. This may be of particular importance where the material is subject to brittle fracture caused by excessive tensile stress.

Appendix: Values of ${}_p\Phi_q$ given by Eq. (50)

$$
\begin{aligned}
{}_1\Phi_1 &= 2[1 + r(\beta - 1)] + 2j + 2k[1 + r(\beta - 1)] + 2lr(\beta - 1) - \xi \\
{}_1\Phi_2 &= [1 + r(\beta - 1)] + (2j + 1) + 2k[1 + r(\beta - 1)] + (2l - 1)r(\beta - 1) - \xi \\
{}_1\Phi_3 &= [1 + r(\beta - 1)] + 2j + 2k[1 + r(\beta - 1)] + 2lr(\beta - 1) - \xi \\
{}_1\Phi_4 &= [1 + r(\beta - 1)] + 2j + 2k[1 + r(\beta - 1)] + (2l - 1)r(\beta - 1) - \xi \\
{}_1\Phi_5 &= [1 + r(\beta - 1)] + 2j + 2k[1 + r(\beta - 1)] + (2l + 1)r(\beta - 1) - \xi \\
{}_1\Phi_6 &= 2j + 2k[1 + r(\beta - 1)] + 2lr(\beta - 1) + \xi \\
{}_1\Phi_7 &= [1 + r(\beta - 1)] + (2j - 1) + 2k[1 + r(\beta - 1)] + (2l + 1)r(\beta - 1) + \xi \\
{}_1\Phi_8 &= [1 + r(\beta - 1)] + 2j + 2k[1 + r(\beta - 1)] + 2lr(\beta - 1) + \xi \\
{}_1\Phi_9 &= [1 + r(\beta - 1)] + 2j + 2k[1 + r(\beta - 1)] + (2l - 1)r(\beta - 1) + \xi \\
{}_1\Phi_{10} &= [1 + r(\beta - 1)] + 2j + 2k[1 + r(\beta - 1)] + (2l + 1)r(\beta - 1) + \xi \\
{}_2\Phi_1 &= [1 + r(\beta - 1)] + 2j + 2k[1 + r(\beta - 1)] + 2lr(\beta - 1) + r\beta - r\xi \\
{}_2\Phi_2 &= [1 + r(\beta - 1)] + 2j + 2k[1 + r(\beta - 1)] + 2lr(\beta - 1) - 1 + r - r\xi \\
{}_2\Phi_3 &= [1 + r(\beta - 1)] + 2j + 2k[1 + r(\beta - 1)] + 2lr(\beta - 1) + 1 + r - r\xi \\
{}_2\Phi_4 &= [1 + r(\beta - 1)] + 2j + 2k[1 + r(\beta - 1)] + 2lr(\beta - 1) + 1 + r\beta - r\xi \\
{}_2\Phi_5 &= [1 + r(\beta - 1)] + 2j + 2k[1 + r(\beta - 1)] + 2lr(\beta - 1) - 1 + r\beta - r\xi \\
{}_2\Phi_6 &= [1 + r(\beta - 1)] + 2j + 2k[1 + r(\beta - 1)] + 2lr(\beta - 1) - r\beta + r\xi \\
{}_2\Phi_7 &= [1 + r(\beta - 1)] + 2j + 2k[1 + r(\beta - 1)] + 2lr(\beta - 1) + 1 - r + r\xi \\
{}_2\Phi_8 &= [1 + r(\beta - 1)] + 2j + 2k[1 + r(\beta - 1)] + 2lr(\beta - 1) - 1 - r + r\xi \\
{}_2\Phi_9 &= [1 + r(\beta - 1)] + 2j + 2k[1 + r(\beta - 1)] + 2lr(\beta - 1) + 1 - r\beta + r\xi \\
{}_2\Phi_{10} &= [1 + r(\beta - 1)] + 2j + 2k[1 + r(\beta - 1)] + 2lr(\beta - 1) - 1 - r\beta + r\xi
\end{aligned}
$$

References

[1] White, R. M., "Generation of Elastic Waves by Transient Surface Heating," *Journal of Applied Physics*, Vol. 34, No. 12, Dec. 1963, pp. 3559–3567.

[2] Zaker, T. A., "Stress Waves Generated by Heat Addition in an Elastic Solid," *Journal of Applied Mechanics*, Vol. 32, Sept. 1965, pp. 143–150.

[3] Morland, L. W., "Generation of Thermoelastic Stress Waves by Impulsive Electromagnetic Radiation," *AIAA Journal*, Vol. 6, No. 6, June 1968, pp. 1063–1066.

[4] Hegemier, G. A. and Morland, L. W., "Stress Waves in a Temperature-Dependent Viscoelastic Half-Space Subjected to Impulsive Electromagnetic Radiation," *AIAA Journal*, Vol. 7, No. 1, Jan. 1969, pp. 35–41.

[5] Goland, M. and Reissner, E., "The Stresses in Cemented Joints," *Journal of Applied Mechanics*, Vol. 11, March 1944, pp. A17–A27.

[6] Payton, R. G., "Bond Stress in Cylindrical Shells Subjected to an End Velocity Step," *Journal of Mathematics and Physics*, Vol. 43, June 1964, pp. 169–190.

[7] Payton, R. G., "Dynamic Bond Stress in a Composite Structure Subjected to a Sudden Pressure Rise," *Journal of Applied Mechanics*, Vol. 32, Sept. 1965, pp. 643–650.

[8] Boley, B. A. and Weiner, J. H., *Theory of Thermal Stresses*, Wiley, New York, 1960.

[9] Gascoigne, H. E., "Transient Stresses in a Layered Thermoelastic Media Generated by Impulsive Energy Deposition," Ph.D. dissertation, 1968, University of Michigan, Ann Arbor, Mich.

[10] Churchill, R. V., *Operational Mathematics*, 2nd edition, McGraw-Hill, New York, 1958, pp. 324–325.